



Calculating the Linearly Polarized Modes and their Properties in Weakly Guiding Step Index Fibers

Rand T. Jameel ^{1*}  and Aqeel R. Salih ² 

^{1,2}Department of Physics, College of Education for Pure Science (Ibn Al-Haitham), University of Baghdad, Baghdad, Iraq

*Corresponding Author

Received: 5/May/2025.

Accepted: 7/August/2025.

Published: 20/January/2026.

doi.org/10.30526/39.1.4166



© 2026 The Author(s). Published by College of Education for Pure Science (Ibn Al-Haitham), University of Baghdad. This is an open-access article distributed under the terms of the [Creative Commons Attribution 4.0 International License](https://creativecommons.org/licenses/by/4.0/)

Abstract

The modal properties of optical fibers were calculated at core radii (1.45–5.05) μm in 1.20 μm increments. In this work, the calculation was performed at a wavelength of 1.030 μm using the RP Fiber Calculator software (free version 2025). The results demonstrated that when the core radius is comparable wavelength, the fiber supports only the fundamental mode, indicating single-mode operation; whereas larger core radii lead to multimode behavior. The study involved analyzing optical properties of step index fibers with core and cladding refractive indices of $n_1 = 1.469$ and $n_2 = 1.46$, respectively. The computed properties included the cut-off wavelength, effective area, power in the core, effective refractive index, and propagation constant. The results revealed a progressive increase in these properties with increasing core radius. Furthermore, the geometric distribution of the modal intensity profiles was visualized to provide a comprehensive understanding of the mode field structure.

Keywords: Step index fibers, RP Fiber Calculator, linearly polarized modes, Weakly guiding fibers.

1. Introduction

Total internal reflection is a fundamental optical phenomenon that directs light within an optical fiber. In its simplest configuration, an optical fiber consists of a cylindrical silica glass core of radius (a) surrounded by a cladding layer that has a lower refractive index (n_2) compared to the refractive index of the core (n_1). This type of fiber is called step index fiber (SIF) due to the abrupt transition in refractive index between the core and the cladding ¹. Optical fibers are classified into two main types based on the number of wave modes propagating within them. Single-mode fibers (SMFs) allow the propagation of only one wave mode. In contrast, multimode fibers (MMFs) support the propagation of multiple wave modes ². The core size is the main factor differentiating the two types of fibers ³. SMFs are important in long-distance communication systems because they provide much greater bandwidth than MMFs ⁴. On the other hand, MMF is more efficient in power transmission applications due to its larger cross-sectional area, making it capable of carrying higher optical power than SMF ⁵. Weakly guiding fibers are defined as optical fibers in which the difference between the refractive indices of the core and cladding is very small, allowing the effects of physical scattering to be separated from scattering due to waveguide properties and facilitating the adoption of simplified and accurate analytical models to describe guided modes ⁶.

In 2015, Aleksandrova calculated a range of modes in weakly guiding MMF and used a wavelength of about 0.633 μm using the BeamProp program ⁷. A study examined the design of SMF via numerical simulations, concentrating on chromatic dispersion and attenuation to optimize C-Band transmission. Employing OptiFiber for Sellmeier equation constants, COMSOL Multiphysics for electromagnetic analysis, and MATLAB for dispersion and

attenuation computations, they attained low attenuation (0.4381 dB/km) and steady dispersion (26.252 ps/nm.km at 1.700 μm), therefore improving optical communication efficiency ⁸. Another study analyzed SMFs and MMFs, highlighting their wide bandwidth and low attenuation for long-distance communication. They examined core radius, numerical aperture, attenuation, and light source effects, comparing SIFs and graded index fibers through theoretical and comparative analysis ⁹. In 2018 a new technique for designing few-mode fiber was developed at a wavelength of 1.550 μm using the COMSOL program ¹⁰. In the same year, were examined linearly polarized (LP) modes and power distribution in double-clad and dispersion flattened SIF by numerical simulations. The researchers examined core power distribution for core radii of 5 μm and 10 μm at (0.850, 1.310, and 1.550) μm wavelengths, discovering a peak core power ratio of 99.4% at 1.550 μm , affected by Fresnel reflection. The research improves comprehension of mode distribution, facilitating the construction of high-efficiency optical fibers to optimize guiding and reduce signal loss via refractive index alterations ¹¹. A study was analyzed mode transfer in SIFs using a three-layer model based on finite element and graphical methods. The results showed that changing the core radius reorganizes the modes between the core and the cladding, supporting LP approximation and promoting advanced fibers' development ¹². In 2020 there was a study designed SMFs using wavelengths (1.310 & 1.550) μm using an RP Fiber Calculator ¹³. In 2021, Shnain computationally analyzed guided modes in SMF and MMFs, confirming the effect of core radius on mode distribution and the increase in maximum values with higher l, m indices. Results were validated using the RP Fiber Calculator ¹⁴. In 2022, were analyzed the relationship between the wavelength and the radius of the core in (SMF & MMFs) at 0.633 μm using an RP Fiber Calculator through a precise and graphical analysis of the intensity of the mode ¹⁵. In 2024, were studied the effect of changing fiber parameters at 1 μm using numerical modelling. The results showed that increasing the radius raises the number of supported modes. At the same time, the refractive index affects the transmission efficiency and reduces power loss, which calls for accurate design to improve the performance of optical communication systems ¹⁶.

In this study, calculations of the modes properties of SMF and MMFs at the wavelength of 1.030 μm were performed utilizing the RP Fiber Calculator software package (free version 2025). In addition, the impact of core radius increasing on these properties was analyzed to determine how this change affects the optical performance of the fibers in this spectral range.

2. Materials and Methods

The performance of optical fibers is influenced by many physical factors, which must be considered when analyzing their optical properties. Among these factors, total internal reflection is a fundamental phenomenon in the propagation of light within an optical fiber, occurring when the angle of incidence is less than the angle of acceptance (θ_a). The following mathematical relationship gives the numerical aperture (NA) of an optical fiber ¹⁷:

$$NA = \sin \theta_a = \sqrt{n_1^2 - n_2^2} \quad (1)$$

The normalized frequency (V) is a critical factor in determining the properties of an optical fiber, as it determines the maximum number of wave modes that can propagate within the core. It can be calculated using the following relationship ¹⁸:

$$V = \frac{2\pi a NA}{\lambda} \quad (2)$$

where λ is the wavelength of the propagating light.

The cut-off wavelength of each mode is given by ¹⁹:

$$\lambda_c = \frac{2\pi a NA}{V_c} \quad (3)$$

where V_c as displayed in **Table 1** is the cut-off frequency of the $LP_{l,m}$ mode.

Table 1. Cut-off V values for the $LP_{l,m}$ modes ¹⁹.

LP modes	V _c
LP _{0,1}	0
LP _{1,1}	2.4048
LP _{2,1}	3.8317
LP _{0,2}	3.8317

For the fundamental mode, the effective area is defined according to the following relationship¹:

$$A_{eff} = \pi\omega^2 \quad (4)$$

The mode radius (ω) can be determined using Marcuse's formula:

$$\omega = (0.65 + 1.619V^{-3/2} + 2.879V^{-6}) a \quad (5)$$

The power in the core is:

$$P \text{ in core} = 1 - \exp(-2 \frac{a^2}{\omega^2}) \quad (6)$$

The propagation constant (β) for each mode is given in terms of the effective refractive index (n_{eff}) and the wavenumber in vacuum ($2\pi/\lambda$) according to the following relationship²⁰:

$$\beta = n_{eff} \frac{2\pi}{\lambda} \quad (7)$$

The effective refractive index (n_{eff}) lies between n_1 and n_2 .

3. Results

This study analyzed the optical fiber wavelength properties using the RP Fiber Calculator software (free version 2025), as shown in **Figure 1**. This software is based on a set of basic inputs, which include the refractive indices of the core and cladding $n_1=1.469$ and $n_2=1.46$, respectively, the radius of the optical fiber core ranging from 1.45 to 5.05 μm and wavelength of 1.030 μm was adopted in the calculations. The program produces a set of fundamental outputs, including the NA and the number of modes, along with other physical properties associated with the wave modes propagating within the optical fiber. The NA value obtained from the software can be validated or compared with those calculated using **Equation (1)**, enabling accurate analysis of the wave properties of the optical fiber. The RP Fiber Calculator evaluated five essential properties of optical modes: the cut-off wavelength, effective mode area, power in the core, effective refractive index and propagation constant. These parameters are important for understanding how light behaves within the fiber and how modes are shaped and guided.

The study started with a fiber core radius of 1.45 μm , a value that has unimodal behavior. The fibers only support the fundamental mode at this dimension. **Table 2** highlights the correspondence between the normalized frequency (V) and the number of supported modes (M). When $V < 2.4048$, the fiber supports just the fundamental mode. As V increases beyond this cut-off, additional modes begin to emerge. Specifically, two modes exist when $2.4048 < V < 3.8317$, and up to four modes are observed in the range $3.8317 < V < 5.1356$.

To better illustrate the relationship between the core radius and the corresponding V and number of supported modes, the data from **Table 2** were plotted graphically in **Figure 2**. These plots provide a clear visual representation of how the normalized frequency and the number of modes evolve as the core radius increases.

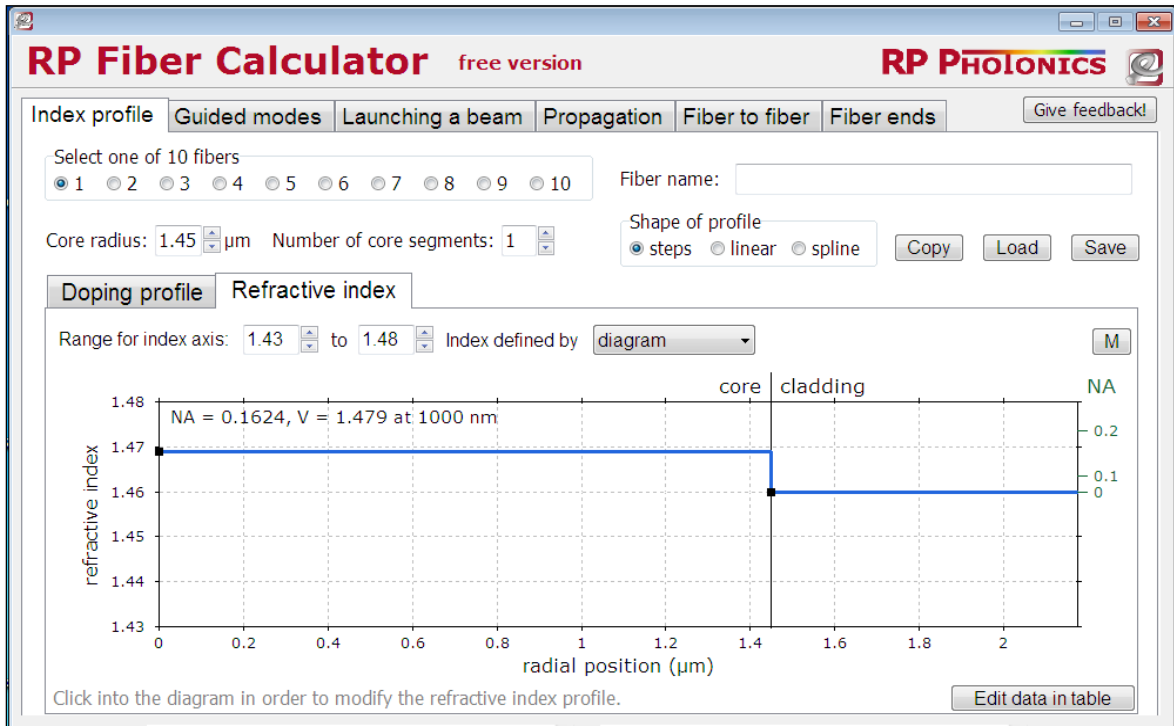


Figure 1. The RP Fiber Calculator interface.

Table 2. V number and fiber modes number.

a (μm)	V from Eq. 2	M from RP program
1.45	1.4365	1
2.65	2.6253	2
3.85	3.8141	2
5.05	5.0029	4

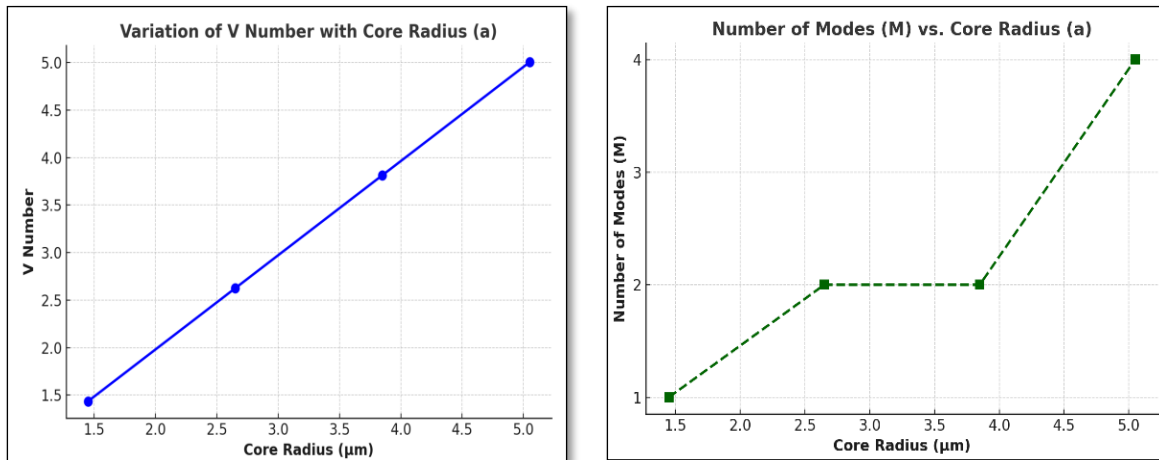


Figure 2. V number and mode count versus fiber core radius.

Tables 3 and 4 report the LP modes cut-off wavelengths in MMFs, obtained through analytical calculation (via Equation 3) and numerical simulation using the RP Fiber Calculator. The fundamental mode does not exhibit a cut-off condition. A high agreement was observed between the cut-off wavelengths derived from the equation and those obtained from the software. It should be noted that all resulting cut-off wavelengths exceed 1.030 μm, as the cut-off frequencies of the modes are lower than the (V) of the fiber.

Table 3. The cut-off wavelengths (μm) at ($a=2.65, 3.85$) μm .

LP modes	a=2.65 μm		a=3.85 μm	
	Eq. 3	RP program	Eq. 3	RP program
LP_{0,1}	No cut-off	No cut-off	No cut-off	No cut-off
LP_{1,1}	1.12443	1.11947	1.63361	1.62640

Table 4. The cut-off wavelengths (μm) at ($a=5.05$) μm .

LP modes	Eq. 3	RP program
LP_{0,1}	No cut-off	No cut-off
LP_{1,1}	2.14278	2.13334
LP_{2,1}	1.34482	1.34171
LP_{0,2}	1.34482	1.34169

Table 5 presents the calculation of the effective area and power in the core for the first mode across a range of values of different core radii based on **Equations (4 and 6)** and compares them with the values obtained from the Calculator. **Tables 6 - 8** illustrate the calculated effective area and power in the core for various modes, based on RP Fiber Calculator results. As the core radius increases, both properties show a noticeable rise. The fundamental mode consistently maintains the highest power confinement among all modes.

Table 5. The (A_{eff}) and (P in core) of all radii (the fundamental mode only).

a (μm)	A_{eff} (μm^2)		P in core	
	Eq. 4	RP program	Eq. 6	RP program
1.45	24.3	20.3	0.419	0.501
2.65	23.8	23.5	0.843	0.860
3.85	35.1	37.4	0.930	0.944
5.05	50.6	56.3	0.958	0.972

Table 6. The (A_{eff}) and (P in core) at ($a=1.45$) μm .

LP mode	A_{eff} (μm^2)	P in core
LP_{0,1}	20.3	0.501

Table 7. The (A_{eff}) and (P in core) at ($a=2.65, 3.85$) μm .

LP modes	a=2.65 μm		a=3.85 μm	
	A_{eff} (μm^2)	P in core	A_{eff} (μm^2)	P in core
LP _{0,1}	23.5	0.860	37.4	0.944
LP _{1,1}	46.8	0.462	38.9	0.830

Table 8. The (A_{eff}) and (P in core) at ($a=5.05$) μm .

LP modes	A_{eff} (μm^2)	P in core
LP_{0,1}	56.3	0.972
LP_{1,1}	53.8	0.921
LP_{2,1}	61.0	0.833
LP_{0,2}	59.1	0.763

The effective refractive index and the propagation constant of the LP_{0,1} mode in an SMF with a core radius of 1.45 μm are presented in **Table 9**, as determined by the RP Fiber Calculator. This substantially impacts the mode's confinement and propagation behavior, as the core radius is approximately equivalent to the operating wavelength. **Tables 10 and 11** display the effective refractive indices and propagation constants for various modes, calculated using the RP Fiber Calculator. The LP_{0,1} mode demonstrates the highest values for both parameters across all analyzed core radii. Furthermore, both (n_{eff}) and (β) exhibit a distinct upward trend as the core radius increase.

Table 9. The (n_{eff}) and (β) at ($a=1.45 \mu\text{m}$).

LP mode	n_{eff}	$\beta (\mu\text{m}^{-1})$
LP _{0,1}	1.461807	8.91728

Table 10. The (n_{eff}) and (β) at ($a=2.65, 3.85 \mu\text{m}$).

LP modes	$a=2.65 \mu\text{m}$		$a=3.85 \mu\text{m}$	
	n_{eff}	$\beta (\mu\text{m}^{-1})$	n_{eff}	$\beta (\mu\text{m}^{-1})$
LP _{0,1}	1.465219	8.93810	1.466789	8.94768
LP _{1,1}	1.460485	8.90922	1.463574	8.92807

Table 11. The (n_{eff}) and (β) at ($a=5.05 \mu\text{m}$).

LP modes	n_{eff}	$\beta (\mu\text{m}^{-1})$
LP _{0,1}	1.467563	8.95240
LP _{1,1}	1.465407	8.93924
LP _{2,1}	1.462683	8.92263
LP _{0,2}	1.461906	8.91789

Table 12. Comparison of the n_{eff} values calculated at a core radius of $5.05 \mu\text{m}$.

LP modes	The present study	Shu and Bass ²¹
LP _{0,1}	1.467563	1.467540
LP _{1,1}	1.465407	1.465350
LP _{2,1}	1.462683	1.462577
LP _{0,2}	1.461906	1.461825

Figures 3 - 6 illustrate the transverse intensity distributions of guided modes at different core radii. For the SMF case (**Figure 3**), the LP_{0,1} mode displays a single central peak with a symmetrical Gaussian-like profile, indicating tight confinement of the optical field in the core due to low V number. As the core radius increases (**Figures 4-6**), additional modes appear with more complex intensity modes, such as dual peaks or multiple lobes.

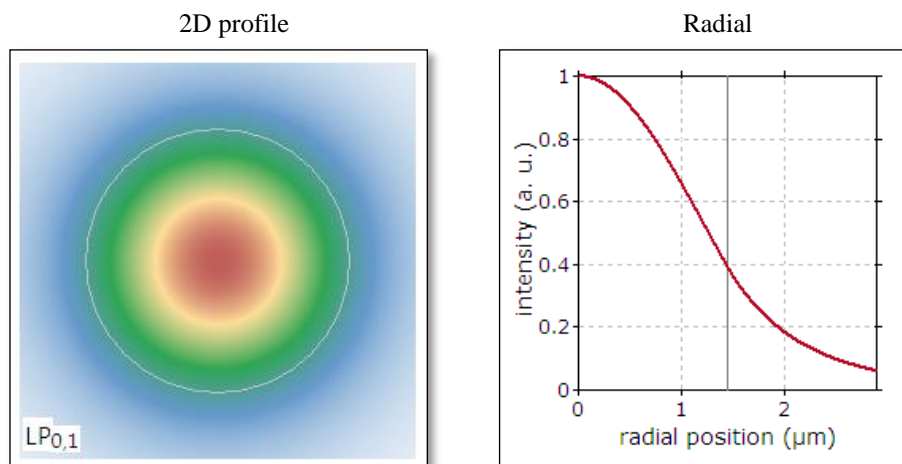


Figure3. The distribution of intensity at ($a=1.45 \mu\text{m}$).

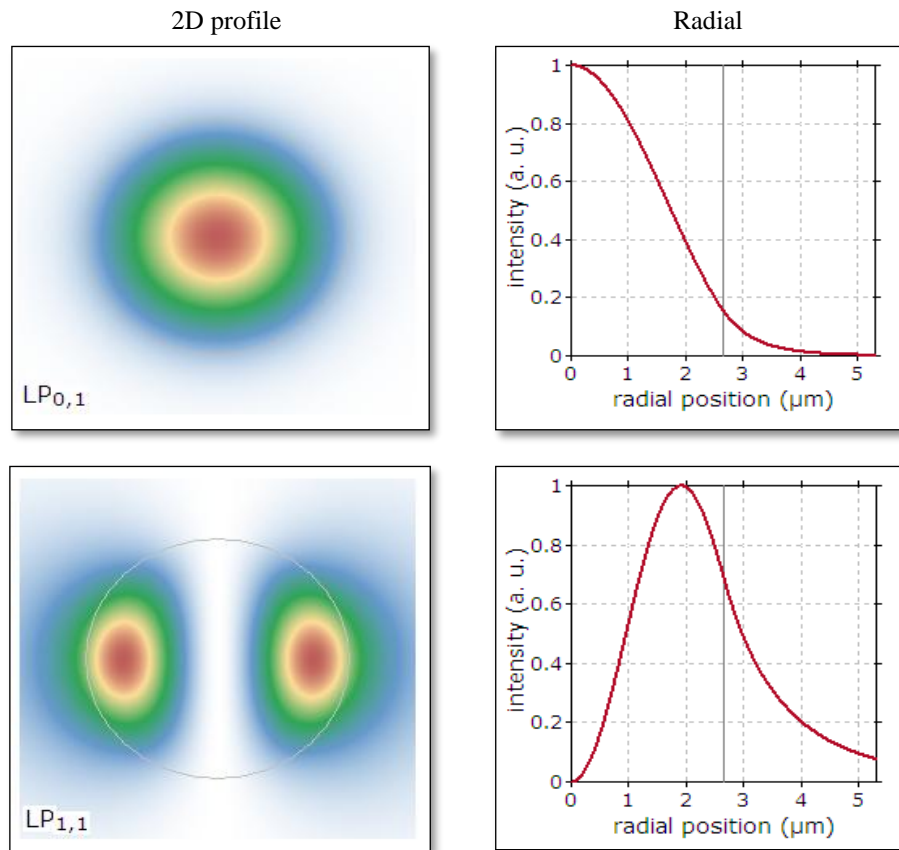


Figure 4. The distribution of intensity at ($a=2.65 \mu\text{m}$).

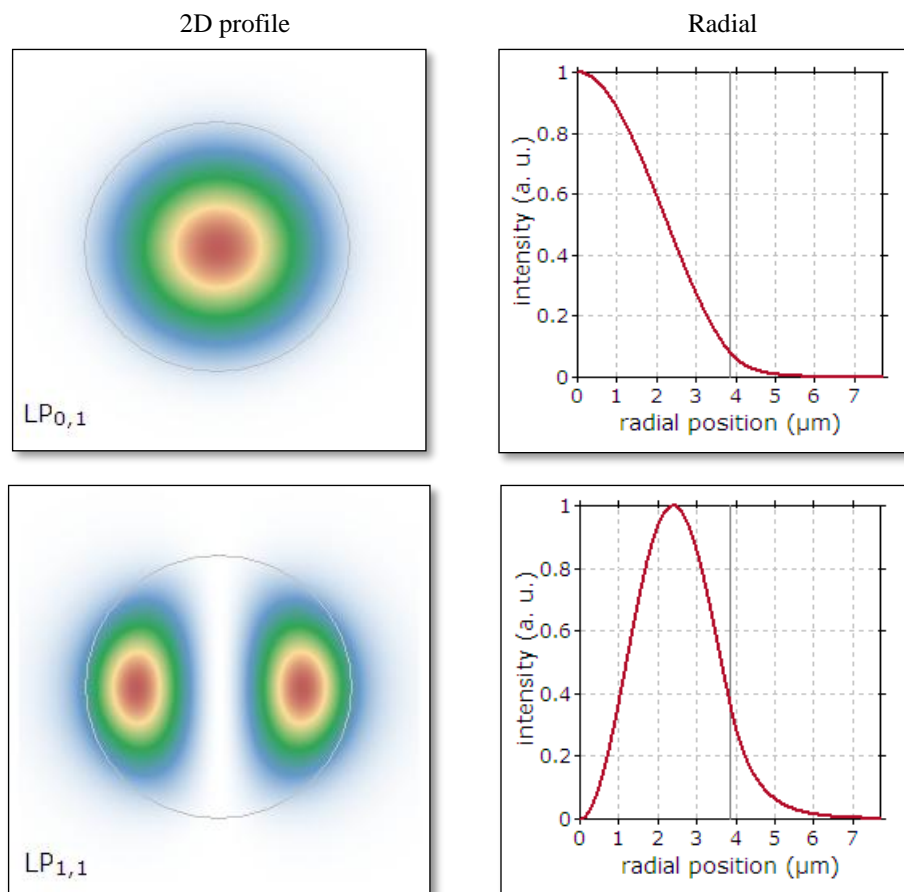


Figure 5. The distribution of intensity at ($a=3.85 \mu\text{m}$).

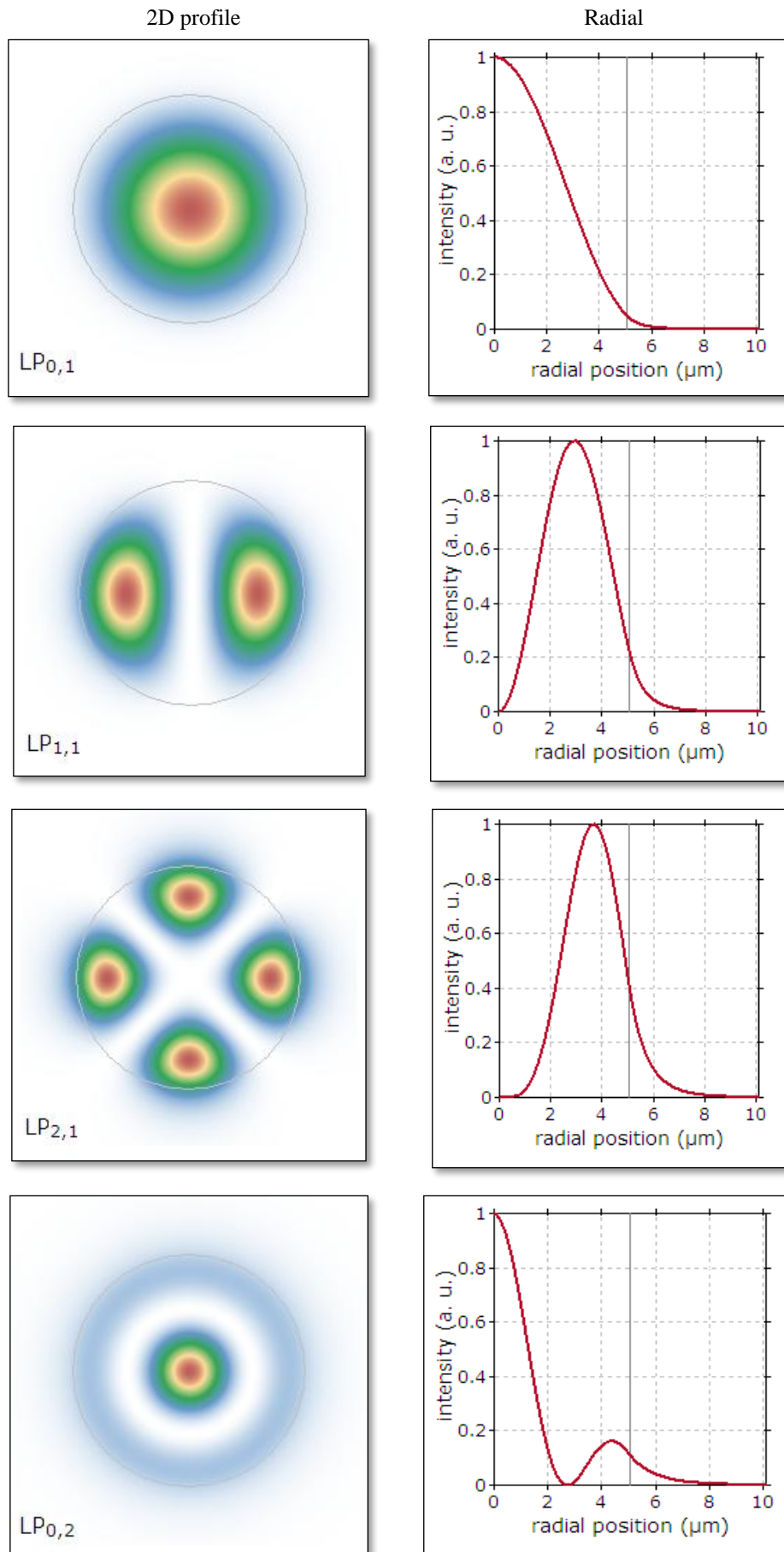


Figure 6. The distribution of intensity at ($a=5.05 \mu\text{m}$).

4. Discussion

The variation in the guided modal properties aligns with the theoretical framework defined by the normalized frequency relation (**Equation 2**). An increase in core radius results in a higher V number, which facilitates the propagation of additional LP modes once their respective cut-off wavelengths are exceeded (**Equation 3**). The values of effective area (**Equation 4**), power confined in the core (**Equation 6**), and effective refractive index (**Equation 7**) exhibit a progressive increase with increasing core radius, confirming the dependency of modes properties on the fiber's geometric parameters. The decrease in the effective refractive index difference between adjacent modes also reflects reduced modal separation, which is characteristic of MMFs and influences dispersion behavior. These analytical interpretations are further supported by a comparison with the numerical study conducted by Shu and Bass²¹, who employed the SD-ID-BPM approach to accurately compute guided modes and their propagation constants as shown in **Table 12**. In contrast, the present study investigated the effect of core radius variation on modal behavior at a wavelength of 1.030 μm using the RP Fiber Calculator. Despite methodological differences, both studies yielded highly consistent results. Furthermore, the present work extended the analysis to include the cut-off wavelength, effective mode area and the proportion of power confined within the fiber core—parameters not considered in the comparative reference. This consistency reinforces the validity of the theoretical expressions adopted and affirms their applicability in describing mode propagation in weakly guiding SIFs.

5. Conclusion

The core radius is critical in determining the optical modes properties supported in an optical fiber. If the core radius is similar to the operating wavelength, the fiber operates in SM, where the optical signal transmission is limited to the fundamental mode only. Conversely, if the core radius is significantly larger than the operational wavelength, the fiber operates in MM, allowing the propagation of multiple optical modes. In this case, the cut-off wavelengths of the different modes exceed the operational wavelength, promoting MMFs. Furthermore, as the radius of the core increases, the physical properties of all supported modes increase, which significantly affects the performance efficiency of optical fibers in signal transmission.

Acknowledgment

First and foremost, I would like to extend my deepest appreciation and gratitude to Dr. Aqeel Razzaq Salih, who has been an essential source of inspiration and support during the various stages of this study. This work was based on many of his outstanding scientific contributions, whether through his research publications or academic theses in the field of optical fibers, which had a great impact on guiding the research path and deepening its content. I would also like to thank the scientists and researchers whose work enriched this study and contributed to strengthening its scientific structure. I also express my deep gratitude to the College of Education for Pure Science (Ibn Al-Haitham) for its fundamental role in my academic career, and for its institutional context that facilitated the publication of this research in an effective and organized manner.

Conflict of Interest

The authors declare that they have no conflicts of interest.

Funding

None.

References

1. Agrawal GP. Fiber-optic communication systems. 5th ed. Hoboken (NJ): Wiley; 2021. 544 p.
2. Tricker R. Optoelectronic and fiber optic standards. In: Optoelectronics and Fiber Optic Technology.

- Elsevier; 2002. p. 263–75. <https://doi.org/10.1016/B978-075065370-1/50012-X>
3. Agrawal GP. Nonlinear fiber optics. In: Nonlinear Science at the Dawn of the 21st Century. Springer; 2000. p. 195–211.
 4. Hill G. The Cable and Telecommunications Professionals' Reference: PSTN, IP and cellular networks, and mathematical techniques. CRC Press; 2012.
 5. Neumann EG. Single-mode fibers: fundamentals. Vol. 57. Springer; 2013.
 6. Gloge D. Dispersion in weakly guiding fibers. Appl Opt. 1971 Nov; 10 (11): 2442–5. <https://doi:10.1364/AO.10.002442.4o>
 7. Aleksandrova AV. Calculation of a mode set in weakly guiding fibers; Computer Optics and Nanophotonics. 2015; 1490: 37–44. <https://doi:10.18287/1613-0073-2015-1490-37-44>
 8. Sakkour D, Dayoub D, Hassan A. Study and design of a single-mode optical fiber (SMF). Tishreen Univ J Res Sci Stud. 2016 Oct; 38: 117-35.
 9. Mohammed SQ, Al-Hindawi AMAM. Study of optical fiber design parameters in fiber optics communications. Kurdistan J Appl Res. 2017; 2 (3): 302-8.
 10. Gulistan A, Ghosh S, Rahman BMA. Enhancement of modal stability through reduced mode coupling in a few-mode fiber for mode division multiplexing. OSA Contin. 2018 Oct 15; 1 (2): 309–19. <https://doi:10.1364/osac.1.000309>
 11. Singh S, Pakhira SA, Brahma D. Study of the linearly polarized modes and power analysis of double-clad refractive index profile of a dispersion flattened step index fiber. In: 2018 International Conference on Applied Electromagnetics, Signal Processing and Communication (AESPC). IEEE; 2018. pp. 1-4. <https://doi:10.1109/AESPC44649.2018.9033374>
 12. Lian X, Farrell G, Wu Q, Han W, Wei F, Semenova Y. Mode transition in conventional step-index optical fibers. In: 2019 18th International Conference on Optical Communications and Networks (ICOON). IEEE; 2019. pp. 1–3. <https://doi:10.1109/ICOON.2019.8934113>
 13. Salih AR. Design of Single Mode Fiber for Optical Communications. Ibn AL-Haitham Journal for Pure and Applied Sciences. 2020; 33 (1): 40–7. <https://doi:10.30526/33.1.2373>
 14. Shnain FA. Design of Optical Fibers and Calculate their Guided Modes Properties at 1550 nm [Master's thesis]. Baghdad, Iraq; 2021.
 15. Hmood WM, Salih AR. Calculation of Modes Properties for Single-Mode and Multimode Fibers at 633 nm. Ibn AL-Haitham Journal for Pure and Applied Sciences. 2022; 35 (4): 55–65. <https://doi:10.30526/35.4.2851>
 16. Ibrahim HK, Salih AR. Studying the effect of changing optical fibers parameters on their modes properties at 1000 nm wavelength. J Phys: Conf Ser. 2024; 2754 (1): 012006. <https://doi:10.1088/1742-6596/2754/1/012006>
 17. Kumar S, Deen MJ. Fiber optic communications: fundamentals and applications. Wiley; 2014.
 18. Gistvik S. Optical Fiber Theory for Communication Networks. 3rd ed. 2004.
 19. Ghatak AK. Optics. New Delhi: Tata McGraw-Hill Higher Education; 2010.
 20. Kawano K, Kitoh T. Introduction to optical waveguide analysis: solving Maxwell's equations and the Schrödinger equation. Wiley; 2001. 275 p.
 21. Shu H, Bass M. Calculating the guided modes in optical fibers and waveguides. Journal of Lightwave Technology. 2007 Sep; 25 (9): 2693–9. <https://doi:10.1109/JLT.2007.902102>